Proceedings of the Korean Nuclear Society Autumn Meeting
Taejon, Korea, October 1999

A Receding Horizon Controller for Nuclear Reactor Power Distribution

Man Gyun Na

Chosun University

375 Seoseok-dong, Dong-gu, Kwangju 501-759, Korea

Abstract

Receding horizon control method is applied to the axial power distribution control in a pressurized water reactor. The basic concept of receding horizon control is to solve *on-line* at each sampling instant an optimization problem for a finite future and to implement the first optimal control input as the current control input. It is a suitable control strategy for time varying systems. The reactor model used for computer simulations is a two-point xenon oscillation model based on the nonlinear xenon and iodine balance equations and a one-group, one-dimensional, neutron diffusion equation having nonlinear power reactivity feedback that adequately describes axial oscillations and treats the nonlinearities explicitly. The reactor core is axially divided into two regions, and each region has one input and one output and is coupled with the other region. Through some numerical simulations, it was shown that the proposed control algorithm exhibits very fast tracking responses due to the step and ramp changes of axial target shape without any residual flux oscillations between the upper and lower halves of the reactor core and also, works well in a time-varying parameter condition.

1. Introduction

Xenon oscillation tends to destabilize the operation of nuclear reactors because the thermal cross section of xenon is extremely large and its effects in the reactor are delayed by the iodine precursor. Xenon distribution in a reactor core can be calculated through changes in the axial and radial power distributions and core reactivity. The fact that there is no direct way of measuring the xenon concentration often causes operators a great deal of difficulty in anticipating the amplitude, direction, and rate of change of the xenon imbalance that is closely related with the axial power shape.

Since the power distribution control has been one of the most challenging control problems in the nuclear field, there have been extensive research activities in this area, especially using conventional optimal control methods [1-9]. The receding horizon control methodology has received much attention as a powerful tool for the control of industrial process systems [10-16]. The receding horizon control method has been applied little in the nuclear field. The basic concept of the receding horizon control is to solve *on-line* an optimization problem for a finite future at current time and to implement the first optimal control input as the current control input. As it were, at the present time the behavior of the process over a horizon is considered. Using a model the process response to changes in the manipulated variable is predicted. The moves of the manipulated variables are selected such that the predicted response has certain desirable characteristics. Only the first computed change in the manipulated variable is implemented. The procedure is then repeated at each subsequent instant. This is its main difference from conventional control that uses a pre-calculated optimal control law. This method presents many advantages over the conventional infinite horizon control because it is possible to handle input and state (or output) constraints in a systematic manner during the design and implementation of the control. In particular, it is a suitable control strategy for time varying systems. Although some tracking controllers use only the current tracking command, the receding horizon control can achieve better tracking performance because future commands are considered in addition to the current tracking command. Therefore, in this work the receding horizon control method is applied to the power distribution control.

In this paper, the reactor core is modeled by being axially divided into two regions. Each region has one input and one output and is coupled with the other region. The controlled process has two inputs and two outputs, and is described by a matrix polynomial model. To implement the proposed algorithm, the partial-length rods are selected as the control actuator to return to the desired power shape.

A two-point (lower and upper halves) xenon oscillation model [17,20] is used for the purpose of computer simulations. The validity of the model was also demonstrated for parameter identification and control purposes [18]. Three different numerical simulations were performed in order to demonstrate the excellent performance of the proposed controller for three cases: (a) track the axial target shape which changes by ramp and step, (b) dampen the oscillations induced by a perturbation, and (c) follow the parameters change.

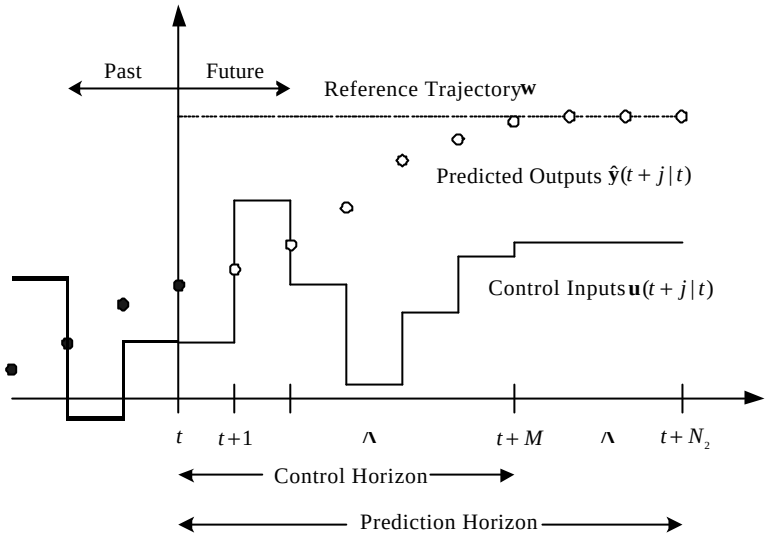

Fig. 1. Receding horizon control method.

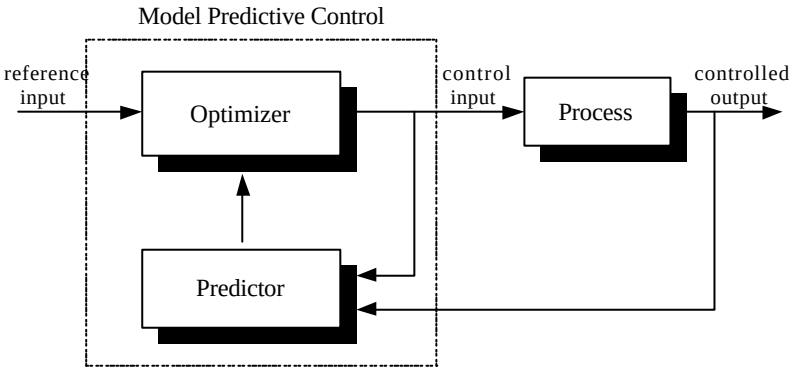

Fig. 2. Schematic diagram of receding horizon control.

2. A Receding Horizon Controller

2.1 Problem Statement

The process to be controlled is described by the following Controlled Auto-Regressive and Integrated Moving Average (CARIMA) model, which is widely used as a mathematical model of control design methods:

$$\mathbf{A}(q^{-1})\mathbf{y}(t) = \mathbf{B}(q^{-1})\mathbf{u}(t-1) + \frac{1}{\Delta}\mathbf{C}(q^{-1})\mathbf{?}(t) \ , \tag{1}$$

where $\mathbf{y} \in R^n$ is the output, $\mathbf{u} \in R^m$ is the control input, $\mathbf{?} \in R^m$ is a stochastic random noise vector sequence with zero mean value, q^{-1} is the backward shift operator, e.g., $q^{-1}\mathbf{y}(t) = \mathbf{y}(t-1)$, and Δ is defined as $\Delta = 1 - q^{-1}$. In Eq. (1), $\mathbf{A}(q^{-1})$ and $\mathbf{C}(q^{-1})$ are $n \times n$ monic matrix polynomials as a function of the backward shift operator q^{-1} and $\mathbf{B}(q^{-1})$ is an $n \times m$ matrix polynomial. For example, the $n \times n$ matrix

polynomial $\mathbf{A}(q^{-1})$ is as follows:

$$\mathbf{A}(q^{-1}) = \mathbf{A}_0 + \mathbf{A}_1 q^{-1} + \mathbf{A}_2 q^{-2} + \mathrm{K} + \mathbf{A}_{nA} q^{-nA} \quad , \tag{2}$$

where $\mathbf{A}_0, \mathbf{A}_1, \Lambda, \mathbf{A}_{nA}$ are $n \times n$ real matrices and nA is the order of the matrix polynomial.

The basic idea of receding horizon control is to calculate a sequence of future control signals in such a way that it minimizes a multistage cost function defined over a prediction horizon. The associated performance index is the following quadratic function:

$$J = \frac{1}{2} \sum_{j=N_1}^{N_2} \left(\hat{\mathbf{y}}(t+j \mid t) - \mathbf{w}(t+j)\right)^T \mathbf{Q} \left(\mathbf{y}(t+j \mid t) - \mathbf{w}(t+j)\right) + \frac{1}{2} \sum_{j=1}^{M} \Delta\mathbf{u}(t+j-1)^T \mathbf{R} \Delta\mathbf{u}(t+j-1) , \tag{3}$$

where positive definite matrices $\mathbf{Q}$ and $\mathbf{R}$ are weighting matrices to penalize particular components of $\left(\hat{\mathbf{y}} - \mathbf{w}\right)$ and $\Delta\mathbf{u}$ at certain future time intervals, respectively, and also, they are symmetric matrices, and $\mathbf{w}$ is a future setpoint or reference sequence for the output vector. $\hat{\mathbf{y}}(t+j \mid t)$ is an optimum j-step ahead prediction of the system output on data up to time t; that is, the expected value of the output vector at time t if the past input and output vectors and the future control sequence are known. N_1 and N_2 is the minimum and maximum prediction horizons, respectively, and M is the control horizon. The prediction horizons mark the limits of the instants in which it is desirable for the output to follow the reference. In order to obtain control inputs it is necessary to minimize the cost function. To do this, the predicted outputs have to be first calculated as a function of past values of inputs and outputs and of future control signals. The control law is imposed by the use of the control horizon concept that consists of considering that after a certain interval $M < N_2$ there is no variation in the proposed control signals, that is: $\Delta\mathbf{u}(t+j-1) = \mathbf{0}$ for $j > M$.

The receding horizon control method is to solve an optimization problem for a finite future at current time and to implement the first optimal control input as the current control input. The procedure is then repeated at each subsequent instant. Figure 1 shows this basic concept [12] and Figure 2 shows a schematic diagram of the receding horizon control method. As it were, for any assumed set of present and future control moves, the future behavior of the process outputs can be predicted over a horizon N_2, and the M present and future control moves ($M \le N_2$) are computed to minimize a quadratic objective function. Though M control moves are calculated, only the first control move is implemented. At the next period, new values of the measured output are obtained, the control horizon is shifted forward by one step, and the same calculations are repeated. The purpose of taking new measurements at each time step is to compensate for unmeasured disturbances and model inaccuracy, both of which cause the system output to be different from the one predicted by the model.

At every time instant, receding horizon control requires the on-line solution of an optimization problem to compute optimal control inputs over a fixed number of future time instants, known as the time horizon. The on-line optimization can be typically reduced to either a linear program or a quadratic program.

II.B. Design of a Receding Horizon Controller

The process output at time $t + j$ can be predicted from the measurements of the output and input up to time step t. The derivation of the optimal prediction is done by solving a Diophantine equation, whose solution can be found by an efficient recursive algorithm. In this derivation, the most usual case when $\mathbf{C}(q^{-1}) = \mathbf{I}_{n \times n}$, will be considered. The j-step-ahead prediction of the multivariable process output is derived below.

Multiplying Eq. (1) by $\Delta\mathbf{E}_j(q^{-1})$ from the left gives

$$\mathbf{y}(t+j) - \mathbf{E}_j(q^{-1})\mathbf{?}(t+j) = \mathbf{F}_j(q^{-1})\mathbf{y}(t) + \mathbf{E}_j(q^{-1})\mathbf{B}(q^{-1})\Delta\mathbf{u}(t+j-1) , \tag{4}$$

where $\mathbf{E}_j(q^{-1})$ and $\mathbf{F}_j(q^{-1})$ are the matrix polynomials satisfying

$$\mathbf{I}_{n \times n} = \mathbf{E}_j(q^{-1})\tilde{\mathbf{A}}(q^{-1}) + q^{-j}\mathbf{F}_j(q^{-1}) , \tag{5}$$

$$\mathbf{E}_j(q^{-1}) = \mathbf{E}_{j,0} + \mathbf{E}_{j,1} q^{-1} + \Lambda + \mathbf{E}_{j,j-1} q^{-(j-1)} , \tag{6}$$

$$\mathbf{F}_j(q^{-1}) = \mathbf{F}_{j,0} + \mathbf{F}_{j,1} q^{-1} + \mathbf{F}_{j,2} q^{-2} + \Lambda + \mathbf{F}_{j,nA} q^{-nA} , \tag{7}$$

and

$$\tilde{\mathbf{A}}(q^{-1}) = \mathbf{A}(q^{-1})\Delta . \tag{8}$$

Equation (5) is called the Diophantine equation and there exist unique matrix polynomials $\mathbf{E}_j(q^{-1})$ and $\mathbf{F}_j(q^{-1})$ of order $j-1$ and nA, respectively such that $\mathbf{E}_{j,0} = \mathbf{I}_{n\times n}$. By taking the expectation operator and considering that $E\{\mathbf{?}(t)\} = 0$, the optimal j-step-ahead prediction of $\hat{\mathbf{y}}(t+j\,|\,t)$ satisfies

$$\hat{\mathbf{y}}(t+j\,|\,t) = \mathbf{F}_j(q^{-1})\mathbf{y}(t) + \mathbf{E}_j(q^{-1})\mathbf{B}(q^{-1})\Delta\mathbf{u}(t+j-1), \tag{9}$$

where $\hat{\mathbf{y}}(t+j\,|\,t) = E\{\mathbf{y}(t+j)|t\}$. $E\{\mathbf{y}(t+j)|t\}$ denotes an estimated value of the output at time step $t+j$ based on all the data up to time step t. The output prediction can easily be extended to the nonzero mean noise case by adding vector $\mathrm{E}_j(q^{-1})E\{\mathbf{?}(t)\}$ to prediction $\hat{\mathbf{y}}(t+j\,|\,t)$.

By making the matrix polynomial $\mathbf{E}_j(q^{-1})\mathbf{B}(q^{-1}) = \mathbf{H}_j(q^{-1}) + q^{-j}\mathbf{H}_{jp}(q^{-1})$ with $d\left(\mathbf{H}_j(q^{-1})\right) < j$, the prediction equation can now be written as

$$\hat{\mathbf{y}}(t+j\,|\,t) = \mathbf{H}_j(q^{-1})\Delta\mathbf{u}(t+j-1) + \mathbf{H}_{jp}(q^{-1})\Delta\mathbf{u}(t-1) + \mathbf{F}_j(q^{-1})\mathbf{y}(t), \tag{10}$$

where $d\left(\mathbf{H}_j(q^{-1})\right)$ denotes the order of polynomial $\mathbf{H}_j(q^{-1})$.

The last two terms of the right hand side of Eq. (10) consist of past values of the process input and output variables and correspond to the free response of the process considered if the control signals are kept constant, while the first term only consists of future values of the control input signal and can be interpreted as the forced response, that is: the response obtained when the initial conditions are zero $\mathbf{y}(t-j) = \mathbf{0}, \Delta\mathbf{u}(t-j) = \mathbf{0}$ for $j = 0, 1, \Lambda$ [16]. Equation (10) can be rewritten as

$$\hat{\mathbf{y}}(t+j\,|\,t) = \mathbf{H}_j(q^{-1})\Delta\mathbf{u}(t+j-1) + \mathbf{f}_j, \tag{11}$$

with $\mathbf{f}_j = \mathbf{H}_{jp}(q^{-1})\Delta\mathbf{u}(t-1) + \mathbf{F}_j(q^{-1})\mathbf{y}(t)$. Then a set of N j-ahead output predictions can be expressed as

$$\hat{\mathbf{y}} = \mathbf{H}\Delta\mathbf{u} + \mathbf{f}, \tag{12}$$

where

$$\hat{\mathbf{y}} = \left[\hat{\mathbf{y}}(t+1\,|\,t)^T \quad \hat{\mathbf{y}}(t+2\,|\,t)^T \quad \Lambda \quad \hat{\mathbf{y}}(t+j\,|\,t)^T \quad \Lambda \quad \hat{\mathbf{y}}(t+N\,|\,t)^T\right]^T,$$

$$\mathbf{H} = \begin{bmatrix} \mathbf{H}_0 & \mathbf{0} & \Lambda & \mathbf{0} & \Lambda & \mathbf{0} \\ \mathbf{H}_1 & \mathbf{H}_0 & \Lambda & \mathbf{0} & \Lambda & \mathbf{0} \\ \mathrm{M} & \mathrm{M} & \mathrm{O} & \mathrm{M} & \mathrm{M} & \mathrm{M} \\ \mathbf{H}_{j-1} & \mathbf{H}_{j-2} & \Lambda & \mathbf{H}_0 & \Lambda & \mathbf{0} \\ \mathrm{M} & \mathrm{M} & \mathrm{M} & \mathrm{M} & \mathrm{O} & \mathrm{M} \\ \mathbf{H}_{N-1} & \mathbf{H}_{N-2} & \Lambda & \Lambda & \Lambda & \mathbf{H}_0 \end{bmatrix},$$

$$\Delta\mathbf{u} = \left[\Delta\mathbf{u}(t)^T \quad \Delta\mathbf{u}(t+1)^T \quad \Lambda \quad \Delta\mathbf{u}(t+j)^T \quad \Lambda \quad \Delta\mathbf{u}(t+N-1)^T\right]^T,$$

$$\mathbf{f} = \left[\mathbf{f}_1^T \quad \mathbf{f}_2^T \quad \Lambda \quad \mathbf{f}_j^T \quad \Lambda \quad \mathbf{f}_N^T\right]^T,$$

and

$$\mathbf{H}_j(q^{-1}) = \sum_{i=0}^{j-1}\mathbf{H}_i q^{-i} .$$

If all initial conditions are zero, the free response $\mathbf{f}$ is zero. If a unit step is applied to the first input at time t; that is, $\Delta\mathbf{u} = [\mathbf{1}\,\mathbf{0}\,\Lambda\,\mathbf{0}]^T$, the expected output sequence $[\hat{\mathbf{y}}(t+1)^T\ \hat{\mathbf{y}}(t+2)^T\ \Lambda\ \hat{\mathbf{y}}(t+N)^T]^T$ is equal to the first column of matrix $\mathbf{H}$. That is, the first column of matrix $\mathbf{H}$ can be calculated as the step response of the plant when a unit step is applied to the first control signal.

The computation of the control input involves the inversion of an $nN_2 \times nN_2$ matrix $\mathbf{H}$ that requires a substantial amount of computation. If the control signal is kept constant after the first M control moves (that is,

$\Delta\mathbf{u}(t+j)=\mathbf{0}_{m\times 1}$ for $j>M$), this leads to the inversion of an $nM\times nM$ matrix that reduces the amount of computation. If so, the set of predictions affecting the cost function can be expressed as

$$\hat{\mathbf{y}}_s=\mathbf{H}_s\Delta\mathbf{u}_s+\mathbf{f}_s, \tag{13}$$

where

$$\hat{\mathbf{y}}_s=\left[\hat{\mathbf{y}}(t+N_1\,|\,t)^T \quad \hat{\mathbf{y}}(t+N_1+1\,|\,t)^T \quad \Lambda \quad \hat{\mathbf{y}}(t+N_2\,|\,t)^T\right]^T,$$

$$\mathbf{H}_s=\begin{bmatrix}\mathbf{H}_{N_1-1} & \mathbf{H}_{N_1-2} & \Lambda & \mathbf{H}_{N_1-M}\\ \mathbf{H}_{N_1} & \mathbf{H}_{N_1-1} & \Lambda & \mathbf{H}_{N_1+1-M}\\ \mathrm{M} & \mathrm{M} & \mathrm{O} & \mathrm{M}\\ \mathbf{H}_{N_2-1} & \mathbf{H}_{N_2-2} & \Lambda & \mathbf{H}_{N_2-M}\end{bmatrix} \text{ with } \mathbf{H}_i=\mathbf{0} \text{ for } i<0,$$

$$\Delta\mathbf{u}_s=[\Delta\mathbf{u}(t)^T\ \Delta\mathbf{u}(t+1)^T\ \Lambda\ \Delta\mathbf{u}(t+M-1)^T]^T,$$

and

$$\mathbf{f}=\left[\mathbf{f}_{N_1}^T \quad \mathbf{f}_{N_1+1}^T \quad \Lambda \quad \mathbf{f}_{N_2}^T\right]^T.$$

The cost function can be rewritten as

$$J=\frac{1}{2}\left(\mathbf{H}_s\Delta\mathbf{u}_s+\mathbf{f}_s-\mathbf{w}_s\right)^T\tilde{\mathbf{Q}}\left(\mathbf{H}_s\Delta\mathbf{u}_s+\mathbf{f}_s-\mathbf{w}_s\right)+\frac{1}{2}\Delta\mathbf{u}_s^T\tilde{\mathbf{R}}\Delta\mathbf{u}_s, \tag{14}$$

where $\mathbf{w}_s=\left[\mathbf{w}_s(t+N_1\,|\,t)^T \quad \mathbf{w}_s(t+N_1+1\,|\,t)^T \quad \Lambda \quad \mathbf{w}_s(t+N_2\,|\,t)^T\right]^T$, $\tilde{\mathbf{Q}}=diag(\mathbf{Q},\Lambda\,,\mathbf{Q})$ is a diagonal matrix that consists of diagonal elements equal to $\mathbf{Q},\Lambda\,,\mathbf{Q}$, and $\tilde{\mathbf{R}}=diag(\mathbf{R},\Lambda\,,\mathbf{R})$. Usually $\tilde{\mathbf{Q}}=\mathbf{I}$ and $\tilde{\mathbf{R}}=\mu\times\mathbf{I}$ are used and m is called an input weighting factor.

The optimal control input can be expressed as

$$\Delta\mathbf{u}_s=\left(\mathbf{H}_s^T\tilde{\mathbf{Q}}\mathbf{H}_s+\tilde{\mathbf{R}}\right)^{-1}\mathbf{H}_s^T\tilde{\mathbf{Q}}\left(\mathbf{w}_s-\mathbf{f}_s\right). \tag{15}$$

Because of the receding control strategy, only $\Delta\mathbf{u}(t)$ is needed at instant t. Thus only the first m rows of the matrix $\left(\mathbf{H}_s^T\tilde{\mathbf{Q}}\mathbf{H}_s+\tilde{\mathbf{R}}\right)^{-1}\mathbf{H}_s^T\tilde{\mathbf{Q}}$ have to be computed.

In order to obtain the control input, it is necessary to calculate the matrix $\mathbf{H}_s$ and the vector $\mathbf{f}_s$. These matrix and vector can be calculated recursively. From now on, the derivation will be described. By taking into account a new Diophantine equation corresponding to the prediction for $\hat{\mathbf{y}}(t+j+1\,|\,t)$, Eq. (5) can also be rewritten as follows:

$$\mathbf{I}_{n\times n}=\mathbf{E}_{j+1}(q^{-1})\tilde{\mathbf{A}}(q^{-1})+q^{-(j+1)}\mathbf{F}_{j+1}(q^{-1}). \tag{16}$$

Subtracting Eq. (5) from Eq. (16) gives

$$\mathbf{0}_{n\times n}=\left[\mathbf{E}_{j+1}(q^{-1})-\mathbf{E}_j(q^{-1})\right]\tilde{\mathbf{A}}(q^{-1})+q^{-j}\left[q^{-1}\mathbf{F}_{j+1}(q^{-1})-\mathbf{F}_j(q^{-1})\right]. \tag{17}$$

Since the matrix $\mathbf{E}_{j+1}(q^{-1})-\mathbf{E}_j(q^{-1})$ is of order j, the matrix can be written as

$$\mathbf{E}_{j+1}(q^{-1})-\mathbf{E}_j(q^{-1})=\tilde{\mathbf{G}}(q^{-1})+\mathbf{G}_j q^{-j}, \tag{18}$$

where $\tilde{\mathbf{G}}(q^{-1})$ is an $n\times n$ matrix polynomial of order smaller or equal to $j-1$ and $\mathbf{G}_j$ is an $n\times n$ real matrix. By substituting Eq. (18) into Eq. (17)

$$\mathbf{0}_{n\times n}=\tilde{\mathbf{G}}(q^{-1})\tilde{\mathbf{A}}(q^{-1})+q^{-j}\left[\mathbf{G}_j\tilde{\mathbf{A}}(q^{-1})+q^{-1}\mathbf{F}_{j+1}(q^{-1})-\mathbf{F}_j(q^{-1})\right]. \tag{19}$$

Since $\tilde{\mathbf{A}}(q^{-1})$ is monic, it is easy to see that $\tilde{\mathbf{G}}(q^{-1})=\mathbf{0}_{n\times n}$. Therefore, from Eq. (18) the matrix $\mathbf{E}_{j+1}(q^{-1})$ can be calculated recursively by

$$\mathbf{E}_{j+1}(q^{-1})=\mathbf{E}_j(q^{-1})+\mathbf{G}_j q^{-j}. \tag{20}$$

The following expressions can easily be obtained from Eq. (19):

$$\mathbf{G}_j=\mathbf{F}_{j,0}, \tag{21}$$

and

$$\mathbf{F}_{j+1,i} = \mathbf{F}_{j,i+1} - \mathbf{G}_j \tilde{\mathbf{A}}_{i+1} \text{ for } i = 0, \Lambda, d(\mathbf{F}_{j+1}) . \tag{22}$$

Also, it can easily be seen that the initial conditions for the recursion equation are given by

$$\mathbf{E}_1 = \mathbf{I}_{n\times n}, \tag{23}$$

and

$$\mathbf{F}_1 = q(\mathbf{I}_{n\times n} - \tilde{\mathbf{A}}) . \tag{24}$$

The vector $\mathbf{f}$ (free response) can be computed by the following recursive relationship:

$$\mathbf{f}_{j+1} = q\left(\mathbf{I} - \tilde{\mathbf{A}}(q^{-1})\right)\mathbf{f}_j + \mathbf{B}(q^{-1})\Delta\mathbf{u}(t+j), \tag{25}$$

with $\mathbf{f}_0 = \mathbf{y}(t)$ and $\Delta\mathbf{u}(t+j) = \mathbf{0}_{m\times 1}$ for $j \geq 0$.

3. Axial Xenon Oscillation Model

An axial xenon oscillation model given in the literatures [17,20] for a pressurized water reactor is used to demonstrate the proposed control algorithm. The two-point model was derived from the nonlinear xenon and iodine balance equations and a one-group, one-dimensional, neutron diffusion equation having nonlinear power reactivity feedback. The total power of the reactor core is held constant even though the power density varies as a function of both time and position. The axial xenon oscillation model will be described below.

The one-dimensional diffusion equation with a prompt-power feedback is

$$D\frac{\partial^2 j(z,t)}{\partial z^2} + \left[\frac{n\Sigma_f}{k} - \Sigma_a(z)\right] j(z,t) - s_X X_0 x(z,t) j(z,t) - a_F \overline{\Sigma}_a f_0 j^2(z,t) = 0, \tag{26}$$

and the iodine and xenon balance equations are

$$\frac{\partial y(z,t)}{\partial t} = \left(g_I \Sigma_f \frac{f_0}{I_0}\right) j(z,t) - l_I y(z,t), \tag{27}$$

and

$$\frac{\partial x(z,t)}{\partial t} = \left(g_I \Sigma_f \frac{f_0}{X_0}\right) j(z,t) + \left(l_I \frac{I_0}{X_0}\right) y(z,t) - l_X x(z,t) - s_X f_0 x(z,t) j(z,t), \tag{28}$$

where the parameters have their usual meanings, and f_0, X_0 and I_0 are the time independent steady-state values of the flux, xenon concentration and iodine concentration, respectively and $j(z,t)$, $x(z,t)$ and $y(z,t)$ are their time varying amplitudes, respectively. The axial coordinate z is measured from the center of the cylinder that is of height H. Two-term spatial, harmonic-series solutions are assumed for the axial flux, xenon, and iodine distributions as follows:

$$j(z,t) = \cos(pz/H) + P(t)\sin(2pz/H), \tag{29}$$

$$x(z,t) = \cos(pz/H) + X(t)\sin(2pz/H), \tag{30}$$

and

$$y(z,t) = \cos(pz/H) + Y(t)\sin(2pz/H). \tag{31}$$

The spatial averages of the fluxand the xenon and iodine concentrations for the lower half of the core are

$$\overline{j}_1(t) = \frac{2}{p}[1 - P(t)], \tag{32}$$

$$\overline{x}_1(t) = \frac{2}{p}[1 - X(t)], \tag{33}$$

and

$$\overline{y}_1(t) = \frac{2}{p}[1 - Y(t)]. \tag{34}$$

The equations for the upper half of the core are

$$\overline{y}_2(t) = \frac{2}{p}[1 + P(t)], \tag{35}$$

$$\bar{x}_2(t) = \frac{2}{p}[1 + X(t)], \tag{36}$$

and

$$\bar{y}_2(t) = \frac{2}{p}[1 + Y(t)]. \tag{37}$$

An equation of the amplitude $P(t)$ is derived and solved by maintaining a reactor as nearly critical as possible using a variational estimate of the eigenvalues of the one-dimensional diffusion equation [17]:

$$-b_b P(t)^2 + 2(b_a - b_c)P(t) + b_b = 0, \tag{38}$$

where

$$b_a = \frac{1}{\Sigma_f}\left[4D\left(\frac{p}{H}\right)^2 + \frac{1}{2}(\Sigma_{a1} + \Sigma_{a2}) + \frac{32}{15p}(s_X X_0 + 3a_F f_0 \overline{\Sigma}_a)\right], \tag{39}$$

$$b_b = \frac{1}{\Sigma_f}\left[\frac{8}{3p}(-\Sigma_{a1} + \Sigma_{a2}) + \frac{64}{15p} s_X X_0 B(t)\right], \tag{40}$$

$$b_c = \frac{1}{\Sigma_f}\left[D\left(\frac{p}{H}\right)^2 + \frac{1}{2}(\Sigma_{a1} + \Sigma_{a2}) + \frac{8}{3p}(s_X X_0 + a_F f_0 \overline{\Sigma}_a)\right], \tag{41}$$

$$I_0 = \frac{g_1 \Sigma_f f_0}{l_I}, \tag{42}$$

$$X_0 = \frac{(g_1 + g_X)\Sigma_f f_0}{l_X + \frac{p}{4} s_X f_0}. \tag{43}$$

The dynamic equations of the other amplitude functions $X(t)$ and $Y(t)$ are obtained by integrating Eqs. (27) and (28) over the two regions of the core and substituting Eqs. (29) through (37) [17,20]:

$$\frac{dY(t)}{dt} = \left(g_I \Sigma_f \frac{f_0}{I_0}\right)P(t) - l_I Y(t), \tag{44}$$

$$\frac{dX(t)}{dt} = \left(g_X \Sigma_f \frac{f_0}{X_0}\right)P(t) + \left(l_I \frac{I_0}{X_0}\right)Y(t) - l_X X(t) - \frac{2}{3} s_X f_0 [P(t) + X(t)]. \tag{45}$$

The detailed axial xenon oscillation model is given in the literature [17].

The one-group diffusion parameters of the foregoing dynamic equations are listed in Table 1. The Σ_a is expressed as the combination of absorption cross sections of the fuel, moderator, structure, and control poison.

Table 1. One-group diffusion parameters of the axial xenon oscillation model [17].

Parameter	Value
f_0	$2.1\times10^{13}\,[cm^{-2}\cdot s^{-1}]$
s_X	$2.6\times10^{-18}\,[cm^2]$
a_F	$3.6\times10^{-16}\,[cm^2\cdot s]$
g_I	0.061
g_X	0.003
g_I	$2.87\times10^{-5}\,[s^{-1}]$
g_X	$2.09\times10^{-5}\,[s^{-1}]$
D	$0.375\,[cm]$
H	$365.8\,[cm]$
Σ_f	$0.65\,[cm^{-1}]$
$n\Sigma_f$	$1.56\,[cm^{-1}]$
$\overline{\Sigma}_a$	$1.523\,[cm^{-1}]$

4. Application to the Axial Xenon Oscillation Model

The two-point xenon oscillation model has two inputs and two outputs that consist of inputs and outputs for the lower and upper halves. Therefore, the control input is obtained from the first two rows of the following equation:

$$\Delta \mathbf{u}_s = \left(\mathbf{H}_s^T \tilde{\mathbf{Q}} \mathbf{H}_s + \tilde{\mathbf{R}}\right)^{-1} \mathbf{H}_s^T \tilde{\mathbf{Q}} \left(\mathbf{w}_s - \mathbf{f}_s\right), \tag{46}$$

where

$$\mathbf{w}_s = \left[w_1(t+N_1) \quad w_2(t+N_1) \quad w_2(t+N_1+1) \quad w_2(t+N_1+1) \quad \Lambda \quad w_1(t+N_2) \quad w_2(t+N_2)\right]^T$$

= the normalized target neutron flux,

$$\Delta \mathbf{u}_s = [\Delta u_1(t) \;\; \Delta u_2(t) \;\; \Delta u_1(t-1) \;\; \Delta u_2(t-1) \;\; \Lambda \;\; \Delta u_1(t+M-1) \;\; \Delta u_2(t+M-1)]^T$$

$$= \begin{bmatrix} \Sigma_{a1}(t) - \Sigma_{a1}(t-1) \\ \Sigma_{a2}(t) - \Sigma_{a2}(t-1) \\ \mathrm{M} \\ \Sigma_{a1}(t+M-1) - \Sigma_{a1}(t+M-2) \\ \Sigma_{a2}(t+M-1) - \Sigma_{a2}(t+M-2) \end{bmatrix}$$

= the variation in absorber cross sections Σ_{a1} and Σ_{a2} between two neighboring time steps,

subscripts '1' or '2' refer to the lower and upper halves of a core, respectively.

Since the nonlinear xenon oscillation model described above is inadequate to design the controller and a linear mathematical model of the xenon oscillation model is used, a linearized model was obtained through the linear identification of the nonlinear xenon oscillation model using a conventional parameter estimation algorithm. The linearized model of Eq. (1) is as follows:

$$\mathbf{A}(q^{-1}) = \begin{bmatrix} 1 & 0 \\ 0 & 1 \end{bmatrix} + \begin{bmatrix} -3.3529 \times 10^{-1} & 4.5865 \times 10^{-1} \\ 1.6992 \times 10^{-1} & -6.2402 \times 10^{-1} \end{bmatrix} q^{-1} + \begin{bmatrix} -1.7591 \times 10^{-1} & 2.9927 \times 10^{-1} \\ 1.0540 \times 10^{-2} & -4.6464 \times 10^{-1} \end{bmatrix} q^{-2}$$
$$+ \begin{bmatrix} -5.0386 \times 10^{-2} & 1.7375 \times 10^{-1} \\ -1.1498 \times 10^{-1} & -3.3912 \times 10^{-1} \end{bmatrix} q^{-3} + \begin{bmatrix} 1.0615 \times 10^{-1} & 1.7217 \times 10^{-2} \\ -2.7151 \times 10^{-1} & -1.8258 \times 10^{-1} \end{bmatrix} q^{-4}$$
$$+ \begin{bmatrix} 2.5033 \times 10^{-1} & -1.2697 \times 10^{-1} \\ -4.1570 \times 10^{-1} & -3.8396 \times 10^{-2} \end{bmatrix} q^{-5} + \begin{bmatrix} 7.5821 \times 10^{-2} & 4.7542 \times 10^{-2} \\ -2.4119 \times 10^{-1} & -2.1291 \times 10^{-1} \end{bmatrix} q^{-6},$$

$$\mathbf{B}(q^{-1}) = \begin{bmatrix} -46.042 & 45.697 \\ 46.043 & -45.696 \end{bmatrix} + \begin{bmatrix} 35.566 & -35.180 \\ -35.565 & 35.181 \end{bmatrix} q^{-1} + \begin{bmatrix} 22.027 & -21.501 \\ -22.026 & 21.502 \end{bmatrix} q^{-2} + \begin{bmatrix} 11.267 & -10.612 \\ -11.266 & 10.613 \end{bmatrix} q^{-3}$$
$$+ \begin{bmatrix} -3.3654 & 3.5666 \\ 3.3663 & -3.5658 \end{bmatrix} q^{-4} + \begin{bmatrix} -17.168 & 16.887 \\ 17.169 & -16.886 \end{bmatrix} q^{-5}.$$

The tuning parameters used in numerical simulations are the prediction horizons N_1 and N_2, the control horizon M, the output and input weighting matrices $\tilde{\mathbf{Q}}$ and $\tilde{\mathbf{R}}$. Increasing the maximum prediction horizon N_2 usually speeds up the step response of the closed loop system but induces an increase in overshoot, and the longer the prediction horizon, the less precise the prediction of the process output. Also, a longer prediction horizon increases the computational burden. Increasing the control horizon usually makes the system more active and hence allows a fast response to the system inputs. However, depending upon the value of the control horizon, the closed loop system response may become oscillatory with a large control horizon. The input weighting factor m of the control sequence plays an important role in determining the behavior of the closed loop system. When the factor decreases, the system can be unstable. As the weighting factor increases, the response become better damped but is slowed down. In all simulations the following parameters are used:

$N = 3$, $M = 2$, $\tilde{\mathbf{Q}} = \mathbf{I}$, and $\tilde{\mathbf{R}} = 10000 \times \mathbf{I}$.

First, a numerical simulation was performed in order to observe the tracking performance of the proposed controller for the axial target flux shape that changes by step or ramp. Figure 3 shows its performance. The normalized target flux is changed by a step increase at $t = 10h$ and by a ramp decrease from $t = 60h$. The proposed controller tracks the target neutron flux without delay.

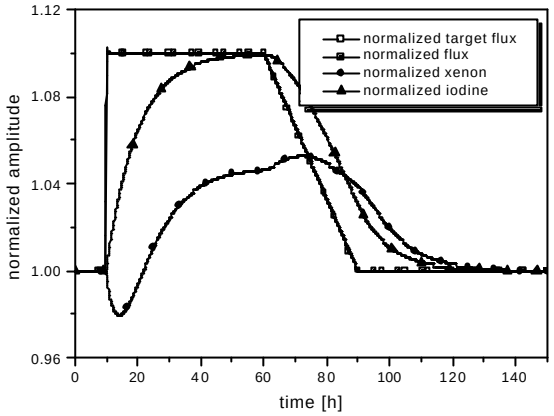

(a) normalized target flux, flux, xenon, and iodine responses at the lower half of the reactor core

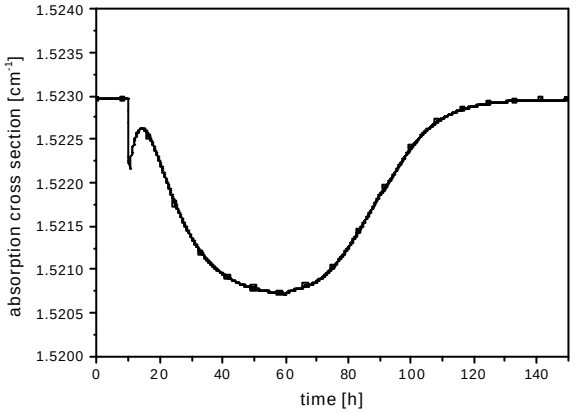

(b) macroscopic cross sections of the absorber in the lower half of the reactor core

Fig. 3. Performance of the proposed controller due to ramp and step changes of axial target shape.

Figure 4 shows how well this controller damps the oscillations when some oscillations are induced externally. A perturbation is initiated at $t = 10h$ suddenly as shown in Fig. 4b and lasts for $2.5h$. Its amount is a 0.2% change of absorber in the lower region at that time. Some free oscillations of the flux, xenon and iodine take place without any controller action for $67.5h$ after the initiation of the perturbation as shown in Fig. 4a. The proposed controller is activated at $t = 80h$ and stops the oscillations promptly. After that time, the normalized neutron flux follows the axial target shape without any delay.

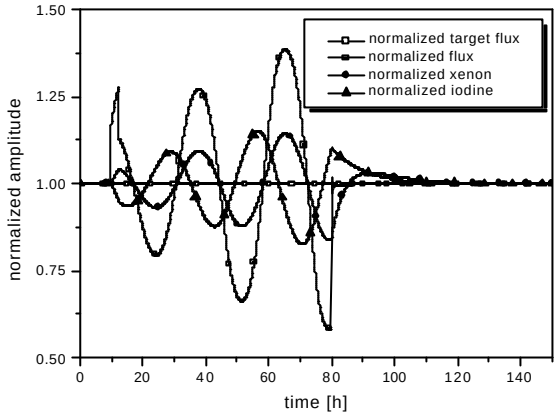

(a) normalized target flux, flux, xenon, and iodine responses at the lower half of the reactor core

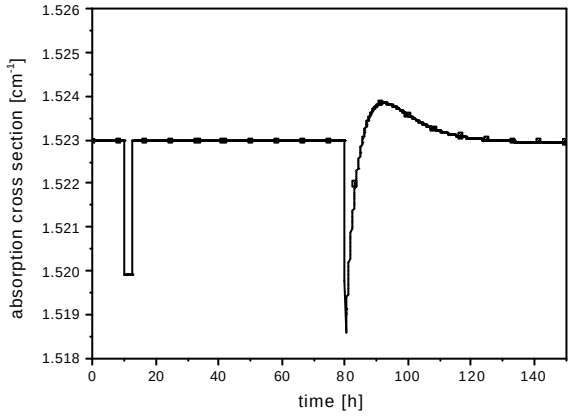

(b) macroscopic cross sections of the absorber in the lower half of the reactor core

Fig. 4. Performance of the proposed controller for the removal of free oscillations.

Figure 5 simulates the circumstances similar to Fig. 3. The difference is that a power reactivity coefficient a_F varies according to a ramp decrease and a step increase as a function of time (refer to Fig. 5c). The parameter value is less than that of the first simulation (refer to Table 1 and Fig. 3). The reactor usually becomes more unstable as the parameter decreases. But its performance is similar to the results of the first numerical simulation.

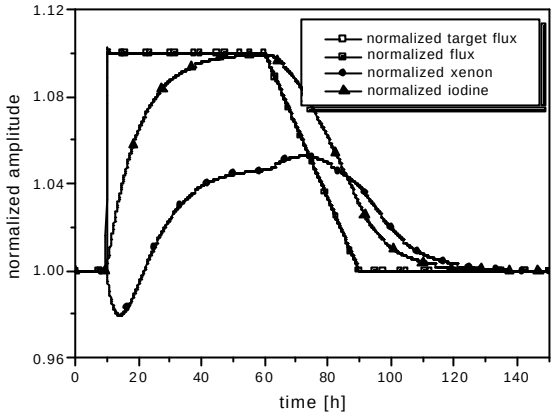

(a) normalized target flux, flux, xenon, and iodine responses at the lower half of the reactor core

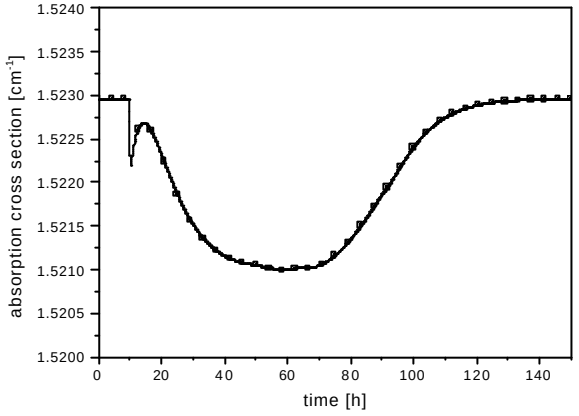

(b) macroscopic cross sections of the absorber in the lower and upper halves of the reactor core

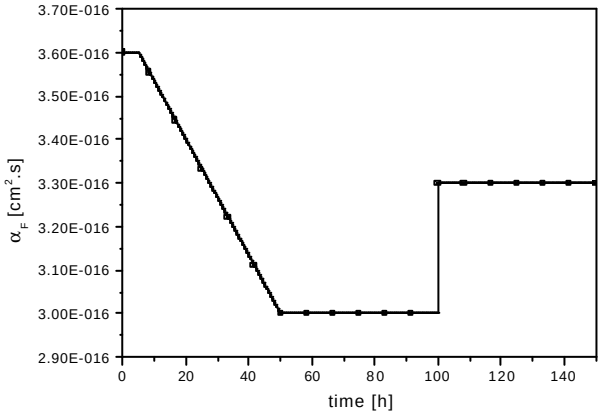

(c) change of the power reactivity coefficient in the reactor core

Fig. 5. Performance of the proposed controller due to ramp and step changes of axial target shape (with parameter change).

5. Conclusions

A receding horizon control algorithm for the axial neutron flux shape control is presented. The concept of receding horizon control is to solve an optimization problem for a finite future at current time and to implement the first optimal control input as the current control input. The procedure is then repeated at each subsequent instant. The proposed algorithm is demonstrated by using a two-point xenon oscillation model based on the nonlinear xenon and iodine balance equations and a one-group, one-dimensional, neutron diffusion equation having nonlinear power reactivity feedback. The proposed control algorithm tracks the step and ramp changes of axial target neutron flux shape without any residual flux oscillations between the upper and lower halves of the reactor core. Also, this controller shows good performance even under time-varying conditions and promptly damps some oscillations induced by external means.

Other computer simulations had been performed under similar circumstances using the same xenon oscillation model and are given in the literatures [19-20]. In the previous works, the reconstructive inverse dynamics control and adaptive control methods had been used. The receding horizon controller shows better response or better characteristics than the controllers of the previous works [19-20].

Acknowledgement

This work was supported by Korea Research Foundation Grant(KRF-99-041-E00460). The author would like to thank the financial support.

References

1. A. M. Christie and C. G. Poncelet, “On the Control of Spatial Xenon Oscillations,” *Nucl. Sci. Eng*., **51**, 21 (1973).
2. S. H. Kim and J. Chang, “Exact Solution for Suboptimal Control of Nuclear Reactors with Distributed Parameters,” *Nucl. Sci. Eng*., **78**, 171 (1981).
3. N. Z. Cho and L. M. Grossman, “Optimal Control for Xenon Spatial Oscillations in Load Follow of a Nuclear Reactor,” *Nucl. Sci. Eng*., **83**, 136 (1983).
4. M. Winokur and L. Tepper, “Extension of Load Power Capability of a PWR Reactor by Optimal Control,” *IEEE Trans. Nucl. Sci*., **NS-31**, 932 (1984).
5. M. H. Yoon and H. C. No, “Direct Numerical Technique of Mathematical Programming for Optimal Control of Xenon Oscillation in Load Following Operation,” *Nucl. Sci. Eng*., **90**, 203 (1985).
6. C. Lin and L. M. Grossman, “Optimal Control of a Boiling Water Reactor in Load-Following via Multilevel Methods,” *Nucl. Sci. Eng*., **92**, 531 (1986).
7. I. A. Gondal and R. A. Axford, “Optimal Xenon Control in Heterogeneous Reactor,” *IEEE Trans. Nucl. Sci*., **NS-33**, 1722 (1986).
8. Gregory D. Wyss and Roy A. Axford, “Multidimensional Effects in Optimal Control Analysis for Nuclear Reactors,” *Nucl. Sci. Eng*., **100**, 458 (1988).
9. Y. H. Park and N. Z. Cho, “A Compensator Design Controlling Neutron Flux Distribution via Observer Theory,” *Annals of Nuclear Energy*, **19**, 513 (1992).
10. W. H. Kwon and A. E. Pearson, “A Modified Quadratic Cost Problem and Feedback Stabilization of a Linear System,” *IEEE Trans. Automatic Control*, **22**, 838 (1977).
11. J. Richalet, A. Rault, J. L. Testud, and J. Papon, “Model Predictive Heuristic Control: Applications to Industrial Processes,” *Automatica*, **14**, 413 (1978).
12. C. E. Garcia, D. M. Prett, and M. Morari, “Model Predictive Control: Theory and Practice – a Survey,”

Automatica, **25**, 335 (1989).

13. M. V. Kothare, V. Balakrishnan, and M. Morari, "Robust Constrained Model Predictive Control Using Linear Matrix Inequality," *Automatica*, **32**, 1361 (1996).
14. J. W. Lee, W. H. Kwon and J. H. Lee, "Receding Horizon H^{∞} Tracking Control for Time-Varying Discrete Linear Systems," *Int. J. Control*, **68**, 385 (1997).
15. J. W. Lee, W. H. Kwon, and J. Choi, "On stability of Constrained Receding Horizon Control with Finite Terminal Weighting Matrix," *Automatica*, **34**, 1607 (1998).
16. Eduardo F. Camacho and Carlos Bordons, *Model Predictive Control*, Springer-Verlag, London (1999).
17. 17. R. J. Onega and R. A. Kisner, "An Axial Xenon Oscillation Model," *Annals of Nuclear Energy*, **5**, 13 (1978).
18. R. J. Onega and R. A. Kisner, "Parameter Identification for Spatial Xenon Transient Analysis and Control," *Annals of Nuclear Energy*, **6**, 369 (1979).
19. R. C. Berkan, B. R. Upadhyaya, L. H. Tsoukalas, and R. A. Kisner, "Reconstructive Inverse Dynamics Control and Application to Xenon-Induced Power Oscillations in Pressurized Water Reactors," *Nucl. Sci. Eng.*, **109**, 188 (1991).
20. Man Gyun Na, B. R. Upadhyaya, J. I. Choi, "Adaptive Control for Axial Power Distribution in Nuclear Reactors," *Nucl. Sci. Eng.*, **129**, 283, (1998).